Inorganic Chemistry
Article

Inorg. Chem. **2010**, *49*, 2649–2655 **2649**
DOI: 10.1021/ic9016195

Redox Induced Electron Transfer in Doublet Azo-Anion Diradical Rhenium(II) Complexes. Characterization of Complete Electron Transfer Series

Nandadulal Paul, Subhas Samanta, and Sreebrata Goswami*

Department of Inorganic Chemistry, Indian Association for the Cultivation of Science, Jadavpur, Kolkata 700 032, India

Received August 13, 2009

Reactions of dirhenium decacarbonyl with the two azoaromatic ligands, L^a = (2-phenylazo)pyridine and L^b = (4-chloro-2-phenylazo)pyridine (general abbreviation of the ligands is L) afford paramagnetic rhenium(II) complexes, $[Re^{II}(L^{\bullet -})_2(CO)_2]$ (**1**) (S = 1/2 ground state) with two one-electron reduced azo-anion radical ligands in an octahedral geometrical arrangement. At room temperature (300 K) the complexes **1a**−**b**, showed magnetic moments (μ_{eff}) close to 1.94 μ_B, which is suggestive of the existence of strong antiferromagnetic interactions in the complexes. The results of magnetic measurements on one of the complexes, **1b**, in the temperature range 2−300 K are reported. The above complexes showed two cathodic and two anodic responses in cyclic voltammetry where one-electron oxidation leads to an unusual redox event involving simultaneous reduction of the rhenium(II) and oxidation of the second ligand via intramolecular electron transfer. The oxidized complexes $\mathbf{1a}^+$ and $\mathbf{1b}^+$ are air stable and were isolated as crystalline solids as their tri-iodide (I_3^-) salts. The structures of the two representative complexes, **1b** and [**1b**]I_3, as determined by X-ray crystallography, are compared. The anionic complexes, $[\mathbf{1}]^-$ and $[\mathbf{1}]^{2-}$ were characterized in solution by their spectral properties.

Introduction

Radicals are the key intermediates[1−3] in several biological processes, organic transformations, small molecule activation, and so forth. Because of its highly reactive nature, stabilization as well as isolation of organic radicals in the pure state is a challenging task. Transition metal complexes of redox active organic ligands have been used[1a,4] for this purpose since such ligands (organic molecules) upon coordination can directly take part in the internal electron transfer processes with the metal center having multivalent possibilities. Consequently, a large variety of transition-metal-stabilized organic radicals has been synthesized in recent years and subjected to detailed investigations.

For example, azoaromatic ligands, owing to the presence of a low lying azo centered vacant π^* molecular orbital, can be populated[5] by one or two electrons chemically or electrochemically resulting in a radical anion and a hydrazido dianion, respectively (Scheme 1).

Though the radical azo-anion oxidation state has been documented in solution[6] for a long time, its isolation in the coordinated state was first reported in 1998. Two examples of azo-anion monoradical complexes[7] of the diamagnetic metal ions Ru(II) and Cu(I) were reported almost simultaneously. Subsequently, singlet diradical complexes of extended azo-aromatic ligands have been reported[8] by us and others in recent years. The radical character of the coordinated azo ligands in the complexes is generally obscured through the coupling of the radical spin with unpaired electrons on the metal or on another radical ligand.

Herein we report two new examples of paramagnetic diradical rhenium(II) complexes coordinated by two azo-anion radical ligands with a non-planar configuration at the metal center. A synthetic strategy with the use of a

*To whom correspondence should be addressed. E-mail: icsg@iacs.res.in.

(1) (a) Chaudhuri, P.; Wieghardt, K. *Prog. Inorg. Chem.* **2001**, *50*, 151. (b) Stubbe, J.; Van der Donk, W. A. *Chem. Rev.* **1998**, *98*, 705. (c) Jadzewski, B. A.; Tolman, W. B. *Coord. Chem. Rev.* **2000**, *200*−*202*, 633.

(2) (a) Mile, B. *Curr. Org. Chem.* **2000**, *4*, 55. (b) Fossey, J.; Lefort, D.; Sorba, J. *Free Radicals in Organic Chemistry*; Wiley: Chichester, U.K., 1995.

(3) (a) Activation and Functionalization of C-H bonds: Heyduk, A. F.; Zhong, H. A.; Lebinger, J. A.; Bercaw, J. E. *ACS Symp. Ser.* **2004**, *885*, 250.

(4) Pierpont, C. G.; Lange, C. W. *Prog. Inorg. Chem.* **1994**, *41*, 331.

(5) Sinan, M.; Panda, M.; Banerjee, P.; Shinisha, C. B.; Sunoj, R. B.; Goswami, S. *Org. Lett.* **2009**, *11*, 3219 and references therein.

(6) (a) Sadler, J. L.; Bard, A. J. *J. Am. Chem. Soc.* **1968**, *90*, 1979. (b) Goswami, S.; Mukherjee, R.; Chakravorty, A. *Inorg. Chem.* **1983**, *22*, 2825.

(7) (a) Shivakumar, M.; Pramanik, K.; Ghosh, P.; Chakravorty, A. *J. Chem. Soc., Chem. Commun.* **1998**, 2103. (b) Shivakumar, M.; Pramanik, K.; Ghosh, P.; Chakravorty, A. *Inorg. Chem.* **1998**, *37*, 5968. (c) Pramanik, K.; Shivakumar, M.; Ghosh, P.; Chakravorty, A. *Inorg. Chem.* **2000**, *39*, 195. (d) Doslik, N.; Sixt, T.; Kaim, W. *Angew. Chem., Int. Ed.* **1998**, *37*, 2403.

(8) (a) Sanyal, A.; Banerjee, P.; Lee, G. -H.; Peng, S. -M.; Hung, C. -H.; Goswami, S. *Inorg. Chem.* **2004**, *43*, 7456. (b) Sanyal, A.; Chatterjee, S.; Castiñeiras, A.; Sarkar, B.; Singh, P.; Fiedler, J.; Záliš, S.; Kaim, W.; Goswami, S. *Inorg. Chem.* **2007**, *46*, 8584. (c) Samanta, S.; Singh, P.; Fiedler, J.; Záliš, S.; Kaim, W.; Goswami, S. *Inorg. Chem.* **2008**, *47*, 1625. (d) Sarkar, B.; Patra, S.; Fiedler, J.; Sunoj, R. B.; Janardanan, D.; Lahiri, G. K.; Kaim, W. *J. Am. Chem. Soc.* **2008**, *130*, 3532. (e) Blanchard, S.; Neese, N.; Bothe, E.; Bill, E.; Weyhermüller, T.; Wieghardt, K. *Inorg. Chem.* **2005**, *44*, 3636.

Published on Web 02/19/2010

Scheme 1

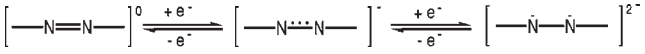

Chart 1

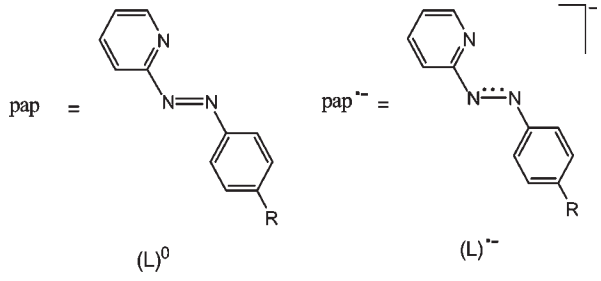

R	L	Complex $[Re(L)_2(CO)_2]$			
		1		$[\mathbf{1}]^+$	
H	L^a	**1a**	$Re^{II}(L^{a\bullet-})_2(CO)_2$	**[1a]**I_3	$[Re^{I}(L^a)_2(CO)_2]I_3$
Cl	L^b	**1b**	$Re^{II}(L^{b\bullet-})_2(CO)_2$	**[1b]**I_3	$[Re^{I}(L^b)_2(CO)_2]I_3$

metal−carbonyl precursor has been developed and successfully applied for isolation of the title complexes. We have also uncovered redox induced electron transfer processes[8c,9,10] in these compounds.

Results and Discussion

Syntheses and Characterization. The two ligands, namely, L^a and L^b, differing with respect to substitution on the phenyl ring, have been used in this work. The isolated compounds are collected in Chart 1.

Reactions[11] of $Re_2(CO)_{10}$ (0.15 mmol) with the ligands (0.61 mmol) (L^a or L^b) in boiling *n*-octane produced new reddish pink $Re^{II}(L^{\bullet-})_2(CO)_2$ complexes (**1a** and **1b**) in 83 and 85% yield, respectively. While selecting Re(0)-carbonyl as the starting compound, it was anticipated that substitution of CO-ligands by L with concomitant internal electron transfer from the electron rich metal Re(0) to the reducible azo aromatic ligand [L] would produce the metal radical complex directly. In line with our synthetic strategy, substitution reaction in $Re_2(CO)_{10}$ by the two L-ligands primarily formed an intermediate complex $Re^0L_2(CO)_2$, which on subsequent internal electron transfer produced the diradical complex, **1**. Our synthetic protocol appears to be more general[8b] and convenient over the available procedure for the synthesis of metal-azoanion radical complexes. A similar reaction[12] of $ReCl(CO)_5$ with L is, however, known to produce a partially CO substituted non-radical complex, $Re^{I}Cl(CO)_3(L)$.

The complexes, **1a** and **1b** gave satisfactory elemental analyses (cf., Experimental Section). Electrospray mass spectra of the complexes corroborate their formulation as $Re(L)_2(CO)_2$. For example, the complex **1a** showed an intense peak due to the molecular ion $[\mathbf{1a}]^+$ at m/z, 609 amu. Notably, the experimental spectral features of the complexes correspond very well to the simulated isotopic pattern for the given formulation. A representative spectrum, that of $[\mathbf{1a}]^+$ along with the simulated spectrum, is submitted as the Supporting Information, Figure S1. Moreover the room temperature magnetic moment μ_{eff} values in the above complexes is nearly 1.94 μ_B, which is much lower[13] than that expected for three uncoupled $S = 1/2$ spins. Accordingly, the electron paramagnetic resonance (EPR) spectrum of **1a** showed a strong single line at $g = 2.003$ with peak to peak line width 308 mT to 343 mT. Notably, the simulated EPR spectrum of **1a** nearly reproduced the observed spectrum, which is submitted as Supporting Information, Figure S2.

The complexes **1a** and **1b** upon oxidation with excess of iodine in dichloromethane solvent produced the cationic complexes $[\mathbf{1a}]I_3$ and $[\mathbf{1b}]I_3$, respectively, in almost quantitative yields. Interestingly, the oxidized complexes possess an $S = 0$ ground state, as determined by magnetic susceptibility measurements at room temperature and are 1:1 electrolytic in acetonitrile (cf. Experimental Section). These displayed sharp ^1H NMR signals in the normal range for diamagnetic compounds. The spectral pattern also reveals that the two ligands in the complexes are magnetically equivalent on the NMR time scale. ^1H NMR spectrum of $[\mathbf{1b}]I_3$ is submitted as the Supporting Information, Figure S3.

X-ray Crystal Structure. The complex (**1b**) of the chloro substituted ligand, L^b, forms dark red crystals, whose structure has been solved by single crystal X-ray diffraction. An Oak Ridge thermal-ellipsoid plot (ORTEP) and atom numbering scheme of the above complex is shown in Figure 1, and selected bond parameters are collected in Table 1. The geometry of the complex is *cis*, *trans* (*ct*) on the basis of relative positions[14] within the pairs N^1, N^1 and N^2, N^2. The N−N distance is an excellent indicator[7,8,15] of the charge on an azo function. From about 1.24 Å for free ligands the coordination by back-donating metals may shift this value to about 1.25−1.30 Å. Real one-electron reduced (i.e., anion radical) ligands have about 1.35 Å while the two-electron reduced hydrazido-(2-) ligands have single bonds with d(N−N) > 1.40 Å. Representative d(N−N) in some known complexes of related azoaromatic ligands are collected[7a−c,11,12,16] in Table 2 for comparison. Similar structure/oxidation state correlations are also available for the complexes of O_2^{n-} ligands[17] and for *o*-quinone-type (1,2-dioxolene)[18] ligands. In the present case the complex **1b** has two ligands with nearly identical d(N−N), namely, 1.345(5) and 1.339(4)Å, suggesting clearly the radical monoanionic

(9) Miller, J. S.; Min, K. S. *Angew. Chem., Int. Ed.* **2009**, *48*, 262 and references therein.
(10) Lu, C. C.; Bill, E.; Weyhermüller, T.; Bothe, E.; Wieghardt, K. *J. Am. Chem. Soc.* **2008**, *130*, 3181.
(11) Lahiri, G. K.; Goswami, S.; Falvello, L. R.; Chakravorty, A. *Inorg. Chem.* **1987**, *26*, 3365.
(12) Sengupta, S.; Panda, B. K. *Transition Met. Chem.* **2005**, *30*, 426.
(13) Ye, S.; Sarkar, B.; Lissner, F.; Schleid, T.; Slageren, V. J.; Fiedler, J.; Kaim, W. *Angew. Chem., Int. Ed.* **2005**, *44*, 2103.
(14) Deb, A. K.; Kakoti, M.; Goswami, S. *J. Chem. Soc., Dalton Trans.* **1997**, 3249.
(15) Muñiz, K.; Nieger, M. *Angew. Chem., Int. Ed.* **2006**, *45*, 2305.
(16) (a) Goswami, S.; Chakravarty, A. R.; Chakrovorty, A. *Inorg. Chem.* **1981**, *20*, 2246. (b) Ghosh, A. K.; Majumdar, P.; Falvello, R. L.; Mostafa, G.; Goswami, S. *Organometallics* **1999**, *18*, 5086.
(17) Cotton, F. A.; Wilkinson, G.; Murillo, C. A.; Bochmann, M. *Advanced Inorganic Chemistry*, 6th ed.; Wiley: New York, 1999; pp 468−471.
(18) Bhattacharya, S.; Gupta, P.; Basuli, F.; Pierpont, G. C. *Inorg. Chem.* **2002**, *41*, 5810.

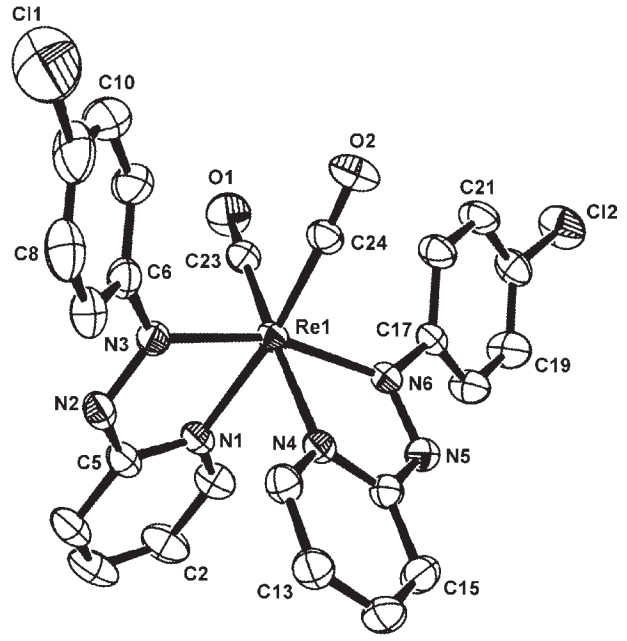

Figure 1. ORTEP representation and atom numbering scheme of the complex **1b**. Hydrogen atoms are omitted for clarity.

Table 1. Selected Bond Distances (Å) and Angles (deg) of **1b** and [**1b**]I_3

	1b	[**1b**]I_3
Re(1)−N(1)	2.139(4)	2.143(6)
Re(1)−N(3)	2.052(3)	2.062(5)
Re(1)−N(4)	2.129(3)	
Re(1)−N(1A)		2.143(6)
Re(1)−N(6)/N(3A)	2.055(3)	
Re(1)−N(3A)		2.062(5)
Re(1)−C(23)	1.914(4)	
Re(1)−C(12)		1.926(8)
Re(1)−C(24)	1.922(5)	
Re(1)−C(12A)		1.926(8)
Re(1)−C(12)/Re(1)−C(12A)		1.926(8)
N(2)−N(3)	1.344(5)	1.305(8)
N(5)−N(6)/N(2A)−N(3A)	1.339(4)	1.305(8)

form of the two coordinated ligands and, by implication, the bivalent state for the metal, $Re^{II}(L^{\bullet-})_2(CO)_2$. The effect of azo bond length elongation in the present complexes is reflected by the lowering of vibrational frequencies $\nu_{N=N}$ as compared to uncoordinated ligand salt $[HL^a]ClO_4$. The $\nu_{N=N}$ band in the uncoordinated $[HL^a]ClO_4$ salt appears[19] at 1437 cm^{-1}, whereas those in the present complexes are considerably lower, appearing at 1190 cm^{-1}. Furthermore, the two intense IR-bands near 1940 and 1875 cm^{-1} are ascribed to $\nu_{C\equiv O}$ and consistent with a mutually *cis*-$(CO)_2$ geometry for the compound. Notably, the CO stretching modes in these complexes are considerably lower in energy than that observed (1985 and 1930 cm^{-1}) in a closely related non-radical complex, $[Re^{I}(CO)_2(L)_2]^+$ (cf. below). Synergistic bonding[20] of the azo anion radical ligands with the strong π-acceptor carbonyl ligands, in part, is responsible for the shift of the $\nu_{C\equiv O}$ to lower frequencies in the diradical complexes, **1a** and **1b**.

The one-electron oxidized form of the rhenium complex **1b** could be crystallized as triiodide, allowing us to establish the N−N bond lengths in the ligands at 1.305(8) Å (cf. Table 1). The ORTEP representation with atom numbering scheme of the compound $[\mathbf{1b}]^+$ is displayed in Figure 2. The coordination geometry of the oxidized complex is similar to that of the reduced complex, **1b**. However, the most striking feature of this structure is the notable contraction of the N−N bond lengths (Table 1). Accordingly the $\nu_{N=N}$ band in [**1**]I_3 appears at a higher frequency (near 1295 cm^{-1}) than that (1190 cm^{-1}) in the corresponding reduced complex. The two intense IR-bands, assigned to CO stretching mode, appear at 1985 and 1930 cm^{-1} in the oxidized complex. Notably, the d(Re−C) in [**1b**]I_3 are longer than that in [**1b**] by 0.08 Å indicating superior Re-CO π back-donation in the diradical complex **1b.**

The bond parameters and the solution properties of the above cationic complex thus indicate the formation of a non-radical complex $[Re^{I}(L)_2(CO)_2]I_3$. One-electron oxidation of the parent complexes **1a** and **1b** results in an oxidatively induced[9,10] simultaneous reduction of the central rhenium(II) ion and oxidation of the second ligand by an intramolecular electron transfer. The redox process is reversible meaning that the reverse transformation, $[\mathbf{1}]^+ \rightarrow \mathbf{1}$, represents a reductively induced oxidation of the central rhenium ion. Redox induced intramolecular electron transfer process in the present case may be explained by invoking the strong preference of an azo chromophore for a low valent metal ion. Thus, the intermediate, $[Re^{II}L(L^{\bullet-})(CO)_2]^+$ formed because of one-electron oxidation of the compound, **1** rapidly undergoes internal electron transfer resulting in the formation of the rhenium(I) complex, $[Re^{I}(L)_2(CO)_2]^+$.

Magnetic Properties. Variable-temperature magnetic susceptibility measurements were performed on a polycrystalline sample of **1b** in the temperature range 2−300 K to assess the magnetic-exchange coupling in the present systems. The temperature dependence of the magnetic behavior ($\chi_M T$ versus T plot, χ_M being the molar magnetic susceptibility) is shown in Figure 3. At 300 K, the value of $\chi_M T$ (0.47 $cm^3\ mol^{-1}\ K$, $\mu_{eff} = 1.94\ \mu_B$) is much lower[13] than that calculated for three uncoupled $S = 1/2$ spins with $g \approx 2$. For **1b**, the antiferromagnetic exchange coupling between low-spin Re^{II} ($S = 1/2$) and two azo-anion radicals ($S = 1/2$) is expected to show a decrease in the magnetic moment with decreasing temperature to attain a μ_{eff} value of 1.73 μ_B at low-temperature. The experimental data show this trend in the temperature range 150−300 K. However, the value of $\chi_M T$ decreases to a very low value of 0.014 $cm^3\ mol^{-1}\ K$ ($\mu_{eff} = 0.32\ \mu_B$) further at 2 K. This behavior is indicative of occurrence of an overall antiferromagnetic interaction in **1b**.

The magnetic behavior of the system may be interpreted considering the exchange-coupling scheme as shown in Figure 4 and using the exchange-Hamiltonian $\hat{H} = -2J(\hat{S}_1\hat{S}_2+\hat{S}_2\hat{S}_3)$ ($S_1 = S_2 = S_3 = 1/2$). From this Hamiltonian it is possible[21a,b] to deduce the following

(19) Saha, A.; Das, C.; Goswami, S. *Indian J. Chem., Sect. A* **2001**, *40A*, 198.

(20) Smithback, J. L.; Helms, J. B.; Schutte, E.; Woessner, S. M.; Sullivan, B. P. *Inorg. Chem.* **2006**, *45*, 2163.

(21) (a) Kahn, O. *Molecular Magnetism*; VCH Publishers: New York, 1993. (b) Brown, D. B.; Wasson, J. R.; Hall, J. W.; Hatfield, W. E. *Inorg. Chem.* **1977**, *16*, 2526. (c) Available through http://ewww/mpi-muelheim.mpg.de/bac/logins/bill/julX_en.php.

Table 2. d(N−N) of Some Known Complexes of [L] and $[L^{\bullet}]^{-}$

non radical azo complexes			Azo anion radical complexes		
compound	N=N length	reference	compound	N···N length	reference
$[HL^{a}]ClO_4$	1.258(5)	19	$[Ru(L^{\bullet-})(PPh_3)_2(CO)Br]$	1.341(17)	7a
$[Re(L^{a})(ArN)Cl_3]$	1.289(5)	11	$[Ru(L^{\bullet-})(PPh_3)_2(CO)Cl]$	1.333(7)	7b
$[Re(L^{a})(CO)_3Cl]$	1.273(4)	12	$[Os(abp^{a\bullet-})(CO)(PPh_3)_2\ Br]$	1.348(22)	7c
$[Ru(L)_2Cl_2]$	1.279(7)	16a	$[Re(L^{b\bullet-})_2(CO)_2]$	1.344(5)	this work
	1.283(6)			1.339(4)	
$[Rh(L)_2Cl_2](ClO_4)$	1.255(5)	16b			
	1.228(5)				
$[Os(L)(H)(CO)(PPh_3)_2]Br$	1.274(13)	7c			
$[Re(L^{b})_2(CO)_2]I_3$	1.305(8)	this work			

[a] abp = 2, 2′ azo bispyridine.

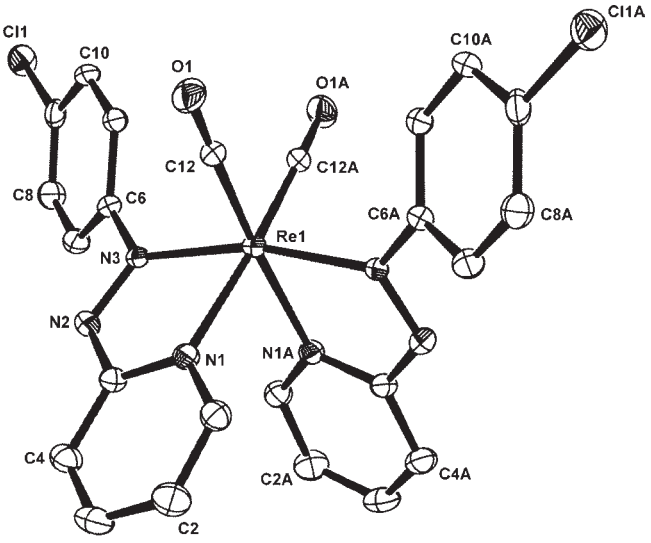

Figure 2. ORTEP representation and atom numbering scheme of the complex [**1b**]I_3. Hydrogen atoms and I_3 are omitted for clarity.

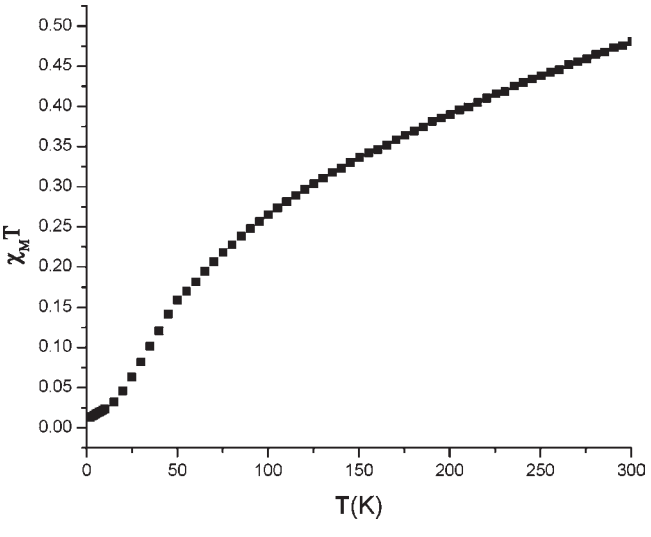

Figure 3. Plot of $\chi_M T$ versus temperature for complex **1b**.

equation for χ_M.

$$\chi_M = \frac{Ng^2\beta^2}{4K(T-\theta)} \cdot \frac{1+\exp(-2J/KT)+10\exp(J/KT)}{1+\exp(-2J/KT)+2\exp(J/KT)}$$

Where the parameters N, g, β, k, θ have their usual meanings, and J is the exchange integral between the central rhenium and two terminal radicals. In the temperature range 150−300 K the experimental data were fitted without considering any intermolecular interaction ($\theta = 0$). The best fit is achieved with $g = 2.003$ (cf. below) and $J = -220\ cm^{-1}$ (Supporting Information, Figure S4, solid red line). However, this could not reproduce the data in the temperature range 2−150 K. A reasonable fitting of the low temperature data was obtained using the intermolecular interaction term θ. Such a fitting yields the parameters: $J = -175\ cm^{-1}$, $g = 2.003$, and $\theta = -65$ K (Supporting Information, Figure S4, solid green line). Our present studies are not enough to understand such a small magnetic moment at 2 K and a highly negative θ value.[22] Further studies are needed for a more definitive conclusion.

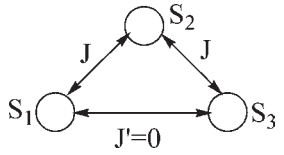

Figure 4. Model for magnetic exchange in **1**.

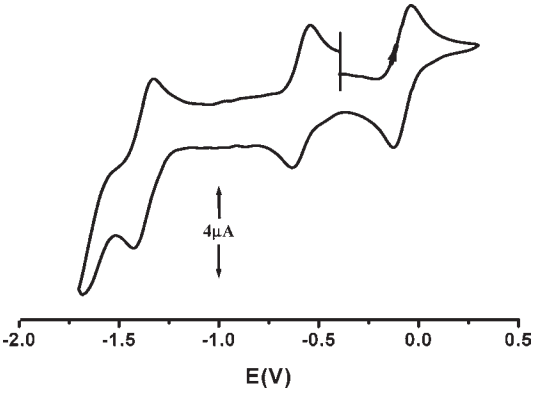

Figure 5. Cyclic voltammogram of **1a** in CH_2Cl_2.

Cyclic Voltammetry and EPR. Cyclic voltammetry of **1a** in CH_2Cl_2 exhibits three reversible (one oxidation and two reductions) one-electron transfer waves at −0.07, −0.58 and −1.37 V, respectively (Figure 5, Supporting Information, Table S1). In addition, an irreversible anodic response was also observed at 1.01 V (Supporting Information, Figure S5). The one-electron redox response has been confirmed by constant-potential electrolysis for the

(22) Imamura, H. *Pure Appl. Chem.* **1986**, *58*, 187.

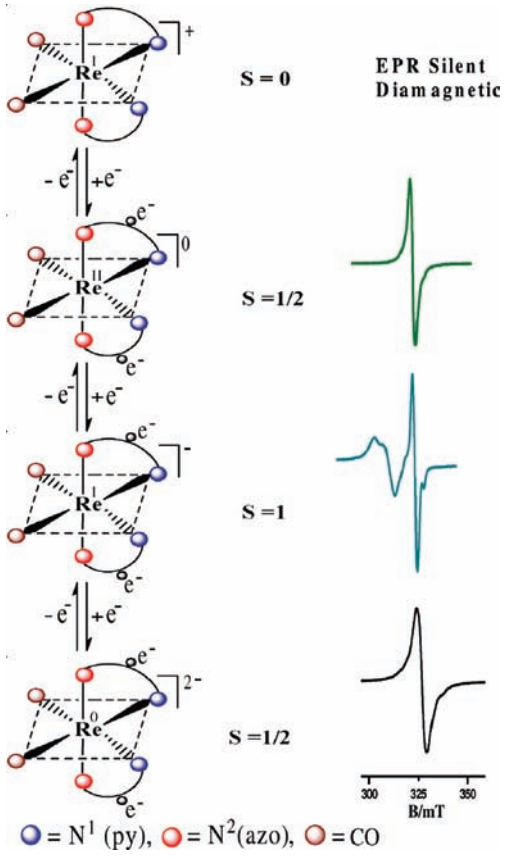

Figure 6. Schematic representation of electron transfer series.

reversible waves at 0.2, −0.8, and −1.6 V, respectively. The redox potentials are found to be sensitive to the nature of substitution on the phenyl ring. Thus, a systematic anodic shift of the redox potentials was observed upon moving from **1a** to **1b** (Supporting Information, Table S1). The first oxidation potential is low and accordingly we have succeeded in isolating the two cationic complexes [**1a**]I_3 and [**1b**]I_3 in a crystalline pure state using I_2 as the oxidizing agent (vide supra). Notably, the reduced complexes **1a** and **1b** can also be regenerated quantitatively from [**1a**]I_3 and [**1b**]I_3, respectively, by the use of hydrazine as reducing agent.

Our attempts to isolate the anionic complexes $[\mathbf{1}]^-$ and $[\mathbf{1}]^{2-}$ were unsuccessful. However, their electronic structures have been examined by EPR measurements of the electrogenerated species (Figure 6). The monoanionic complex, $[\mathbf{1a}]^-$, generated by reductive electrolysis in CH_2Cl_2/0.1 M Bu_4NClO_4 of the compound [**1a**], yielded responses[10,23] typical for a weakly coupled non-planar diradical system. Though we failed to identify the spin forbidden half field signal at $g \approx 4$, satisfactory simulation of the EPR spectrum was obtained by using the following parameters: $g_\perp(1) = 2.228$, $g_\parallel(1) = 2.3850$, $g_\perp(2) = 2.0070$, $g_\parallel(2) = 1.9961$, $A_\perp(1) = 1.0$ mT, $A_\parallel(1) = 5.0$ mT, $A_\perp(2) = 1.0$ mT, $A_\parallel(2) = 5.0$ mT (Supporting Information, Table S2 and Figure S6). This observation points to the reduction of Re^{II} (in **1**) producing a closed cell Re^I ($5d^6$) center (in $[\mathbf{1}]^{1-}$) which acts as a bridge between the two orthogonal azo-anion radical ligands. The diradical situation in the above complex was further probed by the magnetic susceptibility measurement in solution following Evans Method[24] (cf. Supporting Information). The reference monoanion was generated in situ by the addition of one equivalent amount of cobaltocene to [**1a**] in $CDCl_3$ in an inert atmosphere. The effective magnetic moment $\mu_{eff} = 2.43\ \mu_B$ was observed; indicating that the complex $[\mathbf{1a}]^-$ is two electron paramagnetic with weak antiferromagnetic coupling. However, the present experimental data can not totally rule out the contamination of the native oxidized complex (**1a**) in the test solution. The difference of potential between the first and second reduction is high (0.8 V), and we assign the second reductive response to further reduction of Re^I (in $[\mathbf{1}]^{1-}$) to Re^0 (in $[\mathbf{1}]^{2-}$). The dianion $[\mathbf{1a}]^{2-}$ showed a sharp single line EPR spectrum (Supporting Information, Figure S7). This is as expected since the unpaired spin of Re^0 ($5d^7$) in this complex couples with one of the two ligand radicals resulting in a monoradical spin free complex.

Electronic Spectra. UV−visible spectral changes upon stepwise one-electron transfer processes in **1b** are shown in Supporting Information, Figure S8, and the spectral data are collected in Supporting Information, Table S3. Assignments of spectral transitions are guided[8a−c,25] by the available literature on closely related systems.

The complex **1b** displays two major intense bands at 521 and 375 nm (Supporting Information, Table S3) and a broad transition >600 nm. The low energy transitions at 521 nm and the associated shoulder may be assigned to azo-anion radical ligands to the Re(II) transition (LMCT).[8a−c] Upon successive one electron reduction, the ligand-to-metal charge transfer (LMCT) bands shifted slightly to higher energy, and their intensities decreased considerably. Notably, a new weak and broad band also developed near 800 nm in the reduced complexes. One electron oxidation of the complex **1b**, on the other hand, led to redox-induced electron transfer producing the diamagnetic Re^I-compound $[\mathbf{1b}]^+$ of the two neutral azoimine ligands. The spectral features of the oxidized complex are nearly similar to that of the reduced complex, **1b**. The two major transitions occurring at 520 and 372 nm are more intense than those in the reduced complex. The transition at 520 nm may be ascribed as $d\pi(Re) \rightarrow L(\pi^*)$ transition[25] (where $L(\pi^*)$ is believed to be primarily the lowest unoccupied molecular orbital (LUMO) of the azoimine chromophore). The higher energy bands at 372 and 278 nm are due to intra-ligand charge transfer transitions.[8a,25] Absence of any intervalence charge transfer in all of the above complexes is consistent with the electronic descriptions of the systems as described in this paper.

Conclusion. We have reported isolation of two doublet diazoanion radical complexes of rhenium(II) from electron rich $Re^0_2(CO)_{10}$. Multiple electron transfer in it allowed us to isolate or identify the following species: $[Re^I(L)_2(CO)_2]^+$ $[\mathbf{1}]^+$, $[Re^{II}(L^{\bullet-})_2(CO)_2]$ [**1**], $[Re^I(L^{\bullet-})_2(CO)_2]^-$ $[\mathbf{1}]^-$, and $[Re^0(L^{\bullet-})_2(CO)_2]^{2-}$ $[\mathbf{1}]^{2-}$. The transformation $\mathbf{1} \rightleftharpoons \mathbf{1}^+$ occurs via a redox induced reversible double electron transfer

(23) Gastel, M. V.; Lu, C. C.; Wieghardt, K.; Lubitz, W. *Inorg. Chem.* **2009**, *48*, 2626.

(24) (a) Evans, D. F. *J. Chem. Soc.* **1959**, 2003. (b) Philips, W, D.; Poe, N. *Methods Enzymol.* **1972**, *24*, 304. (c) Schubert, E. M. *J. Chem. Educ.* **1992**, *69*, 62.

(25) Samanta, R.; Munshi, P.; Santra, B. K.; Loknath, N. K.; Sridhar, M. A.; Prasad, J. S.; Lahiri, G. K. *J. Organomet. Chem.* **1999**, *579*, 311 and references therein.

Table 3. Crystallographic Data of [**1b**] and [**1b**]I_3

	1b	[**1b**]I_3
empirical formula	$C_{24}H_{16}Cl_2N_6O_2Re$	$C_{24}H_{16}Cl_2N_6O_2ReI_3$
molecular mass	677.58	1058.00
temperature (K)	293(2)	293(2)
crystal system	monoclinic	monoclinic
space group	*C*2/*c*	*C*2/*c*
a (Å)	25.248(2)	8.6584(8)
b (Å)	11.6185(9)	25.702(2)
c (Å)	19.4847(16)	16.3585(16)
α (deg)	90	90
β (deg)	120.659(2)	120.703(3)
γ (deg)	90	90
V (Å^3)	4916.8(7)	3551.3(6)
Z	8	4
D_{calcd} (g/cm^3)	1.831	1.979
cryst. dimens. (mm)	0.07 × 0.17 × 0.20	0.07 × 0.15 × 0.24
θ range for data coll (deg)	1.9−31.7	1.6−29.3
GOF	1.01	0.74
reflns. collected	37419	24263
unique reflns.	7448	4794
largest diff. between peak and hole (e Å^{-3})	1.28, −0.97	3.12, −2.85
final *R* indices [$I > 2\sigma(I)$	R1 = 0.0309 wR2 = 0.0720	R1 = 0.0445 wR2 = 0.1356

process. This redox induced electron transfer process has been followed by the isolation and characterization of the complex [**1**]I_3. Notably, the oxidation state of Re in the two complexes $\mathbf{1}^+$ and $\mathbf{1}^-$ is identical but that of the coordinated azo-ligands is different. Thus, while $\mathbf{1}^+$ is diamagnetic, its redox partner $\mathbf{1}^-$ is a weakly coupled diradical system. We are in search of suitable triradical complexes of L and related non-innocent ligands to examine structure-oxidation state correlation.

Experimental Section

Materials. The metal carbonyl $Re_2(CO)_{10}$ is an Aldrich reagent, and *n*-octane was obtained from Spectrochem India. The ligands L^a and L^b were prepared by following the reported procedure.[26] Tetraethylammoniumperchlorate was prepared and recrystallized as reported earlier.[27] ***Caution!*** *Perchlorates have to be handled with care and appropriate safety precautions.* All other chemicals and solvents were of reagent grade and used as received.

Instrumentation. UV−vis−NIR absorption spectra were recorded on a Perkin-Elmer Lambda 950 UV/vis spectrophotometer and a J&M TIDAS instrument. ^{1}H NMR spectra were taken on a Bruker Advance DPX 300 spectrometer, and $SiMe_4$ was used as the internal standard. Infrared spectra were obtained using a Perkin-Elmer 783 spectrophotometer. Cyclic voltammetry was carried out in 0.1 M Bu_4NClO_4 solutions using a three-electrode configuration (platinum working electrode, Pt counter electrode, Ag/AgCl reference) and a PC-controlled PAR model 273A electrochemistry system. A Perkin-Elmer 240C elemental analyzer was used to collect microanalytical data (C, H, N). ESI mass spectra were recorded on a micro mass Q-TOF mass spectrometer (serial no. YA 263). EPR spectra in the X band were recorded with a JEOL JES-FA200 spectrometer, and the EPR simulations were done using the software provided with it. Magnetic susceptibilities of the polycrystalline sample (**1b**) were recorded on a SQUID magnetometer (MPMS, Quantum Design) in the temperature range 2−300 K with an applied field of 1000 Oe. Magnetic moment measurements for $[\mathbf{1a}]^+$ and $[\mathbf{1b}]^+$ were carried out with a PAR 155 vibrating sample magnetometer fitted with a Walker Scientific L75FBAL magnet, and magnetic susceptibility measurements of the chemically generated samples $[\mathbf{1a}]^-$ and $[\mathbf{b}]^-$ were made using the Evans method[24] with a Bruker Advance DPX 300 spectrometer at 298 K (details are submitted as Supporting Information). Experimental susceptibilities data were corrected for the underlying diamagnetism using Pascal's constant. Simulation and analysis of magnetic susceptibility data were made using the program julX written by E. Bill calculating through full-matrix diagonalization of the Spin-Hamiltonian.[21c] Electrical conductivities were measured by using a Systronics Direct Reading Conductivity meter 304.

Synthesis of $Re^{II}(L^{a\bullet-})_2(CO)_2$ 1a. A 100 mg portion of Re_2CO_{10} (0.15 mmol) and 134 mg of L (0.61 mmol) were refluxed in *n*-octane for 72 h. The color of the solution changes from orange to reddish pink. The crude complex was crystallized from hot *n*-octane solution of the reaction mixture. Yield: 83%. IR (KBr, cm^{-1}): 1185 [ν(N═N)]; 1875, 1940 [ν(C≡O)]. UV−vis (dichloromethane), λ_{max}/nm(ε/M^{-1} cm^{-1}): 652sh, 530(7215), 381(22785), 287sh. ESI-MS, *m*/*z*: 609 [M]$^+$. Anal. Calcd for $C_{24}H_{18}N_6O_2Re$: C, 47.36; H, 2.98; N, 13.81 Found: C, 47.33; H, 3.01; N, 13.79.

Synthesis of $Re^{II}(L^{b\bullet-})_2(CO)_2$ 1b. The compound **1b** was synthesized similarly as above. The yield and characterization data are as follows: Yield: 85%. IR (KBr, cm^{-1}): 1190 [ν(N═N)]; 1875, 1940 [ν(C≡O)]. UV−vis (dichloromethane), λ_{max}/nm(ε/M^{-1} cm^{-1}): 648sh, 521 (6970), 375 (22590), 285sh. ESI-MS, *m*/*z*: 677 [M]$^+$. Anal. Calcd for $C_{24}H_{16}C_{l2}N_6O_2Re$: C, 42.54; H, 2.38; N, 12.40 Found: C, 42.51; H, 2.35; N, 12.36.

Synthesis of $[Re^I(L^a)_2(CO)_2]I_3$ [1a]I_3. To a solution of 50 mg (0.05 mmol) of **1a** in 10 mL of dichloromethane, a slight excess solution, 30 mg (0.11 mmol) of iodine in the same solvent was added dropwise. The solution turned brown, and the solvent was evaporated in a rotary evaporator. The crude product, thus obtained, was thoroughly washed with hexane to remove excess iodine and was crystallized by slow diffusion of a dichloromethane solution into hexane. Yield: 94% IR (KBr, cm^{-1}): 1295 [ν(N═N)], 1930, 1985 [ν(C≡O)]. UV−vis (dichloromethane), λ_{max}/nm(ε/M^{-1} cm^{-1}): 642sh, 527(10150), 377 (32165), 280sh. ESI-MS, *m*/*z*: 609 [M]$^+$. Molar Equivalent Conductance Λ(CH_3CN): 136 Ω^{-1} cm^2 M^{-1}. Anal. Calcd. for $C_{24}H_{18}N_6O_2ReI_3$: C, 29.14; H, 1.83; N, 8.49. Found: C, 29.12; H, 1.87; N, 8.46.

Synthesis of $[Re^I(L^b)_2(CO)_2]I_3$ [1b]I_3. The compound **1b** was synthesized similarly as above. The yield and characterization data are as follows: Yield: 96% IR (KBr, cm^{-1}): 1295 [ν(N═N)], 1930, 1985 [ν(C≡O)]. UV−vis (dichloromethane), λ_{max}/nm(ε/M^{-1} cm^{-1}): 639sh, 520 (10087), 372 (31925), 278sh. *m*/*z*: 677 [M]$^+$. Molar Equivalent Conductance, Λ(CH_3CN): 140 Ω^{-1} cm^2 M^{-1}. Anal. Calcd. for $C_{24}H_{16}Cl_2N_6O_2ReI_3$: C, 27.24; H, 1.52; N, 7.94. Found: C, 27.22; H, 1.54; N, 7.91.

Regeneration of **1a** and **1b** from [**1a**]I_3 and [**1b**]I_3 can be achieved by the addition of a dilute aqueous solution of N_2H_4 to the acetonitrile solution of [**1a**]I_3 and [**1b**]I_3, respectively. The spectra and other properties of **1a** and **1b**, thus obtained, match exactly with the authentic sample.

Crystallography. Crystallographic data for the compounds **1b**, and [**1b**]I_3 are collected in Table 3. Suitable X-ray quality crystals of these are obtained as follows: **1b**, by slow cooling of a hot *n*-octane solution of the compound and [**1b**]I_3; by slow evaporation of a dichloromethane-hexane solution of the compound.

All data were collected on a Bruker SMART APEX-II diffractometer, equipped with graphite monochromated Mo Kα radiation (λ = 0.71073 Å), and were corrected for Lorentz-polarization effects. **1b**: A total of 37419 reflections were collected, of which 7448 were unique (R_{int} = 0.037), satisfying the ($I > 2\sigma(I)$) criterion, and were used in subsequent analysis.

(26) Campbell, N.; Henderson, A. W.; D. Taylor, D. J. *J. Chem. Soc.* **1953**, 1281.
(27) Goswami, S.; Mukherjee, R. N.; Chakravarty, A. *Inorg. Chem.* **1983**, *22*, 2825.

[**1b**]I_3: A total of 24263 reflections were collected, of which 4794 were unique (R_{int} = 0.055).

The structures were solved by employing the SHELXS-97 program package[28] and were refined by full-matrix least-squares based on F^2 (SHELXL-97).[29] All hydrogen atoms were added in calculated positions. Few numbers of diffused scattered peaks were observed in the complex [**1b**]I_3 which can be attributed to disordered solvent molecule. Attempts to model these peaks were unsuccessful because of the diffused nature of the residual electron densities. PLATON/SQUEEZE[30] was used to refine the structure further. A total potential solvent accessible area volume of 213.00 Å^3 per unit cell was found.

(28) Sheldrick, G. M. *Acta Crystallogr., Sect. A* **1990**, *46*, 467.
(29) Sheldrick, G. M., *SHELXL 97. Program for the refinement of crystal structures*; University of Göttingen; Göttingen, Germany, 1997.
(30) Spek, A. L. *PLATON for MS-Windows*, *J. Appl. Crystallogr.* **2003**, *36*, 7.

Acknowledgment. The research was supported by the Department of Science and Technology, India (Project SR/S1/IC- 24/2006). We are grateful to the reviewers for their suggestions at the revision stage. We are thankful to Professor R. Mukherjee, IITK, and Dr. T. K. Paine, IACS, for their help in analyzing the cryomagnetic data. Crystallography was performed at the DST-funded National Single Crystal Diffractometer Facility at the Department of Inorganic Chemistry, IACS. S.S. is thankful to the Council of Scientific and Industrial Research for fellowship support.

Supporting Information Available: X-ray crystallographic files in CIF format for **1b** and [**1b**]$^+$, cyclic voltammogram of **1a**, ^{1}H NMR spectrum of the complex [**1b**]I_3, and UV−vis spectra of **1b**, [**1b**]$^+$, [**1b**]$^-$, and [**1b**]$^{2-}$, observed as well as simulated EPR spectra of **1a**, [**1a**]$^-$, [**1a**]$^{2-}$, experimental as well as the simulated $\chi_M T$ versus T plot are provided. This material is available free of charge via the Internet at http://pubs.acs.org.